The Journal of Veterinary Medical Science

NOTE

Surgery

Low-field magnetic resonance imaging and computed tomography of a calf with aqueductal stenosis caused by web: comparison with normal calves

Ai HORI[1)], Kazuyuki SUZUKI[2)], Masateru KOIWA[2)], Kenjirou MIYOSHI[1)] and Tetsuya NAKADE[1)]*

[1)]Department of Small Animal Clinical Sciences, School of Veterinary Medicine, Rakuno Gakuen University, 582-1 Bunkyoudai-Midorimachi, Ebetsu, Hokkaido 069-8501, Japan
[2)]Department of Large Animal Clinical Sciences, School of Veterinary Medicine, Rakuno Gakuen University, 582-1 Bunkyoudai-Midorimachi, Ebetsu, Hokkaido 069-8501, Japan

J. Vet. Med. Sci.
81(1): 42–47, 2019
doi: 10.1292/jvms.18-0020

Received: 17 January 2018
Accepted: 31 October 2018
Published online in J-STAGE: 14 November 2018

ABSTRACT. A 6-day-old female Holstein displayed a dome-shaped skull and cardiac murmur on physical examination. Neurological abnormalities included progressive ataxia, decreased pupillary light reflex, and blindness soon after birth. On diagnostic imaging, CT identified expanded ventricles and thyroid hypoplasia on the left side. MRI detected expanded ventricles, especially in the rostral cerebrum at the mesencephalic aqueduct, compared with normal calves, so we suspected hydrocephalus causing stenosis of the mesencephalic aqueduct. Postmortem examination revealed a structure in the mesencephalic aqueduct resembling the "web" type of aqueductal stenosis described in humans. This case report indicates the utility of describing mesencephalic aqueductal stenosis by web and detection of other malformations on CT and MRI for antemortem diagnosis in calves.

KEY WORDS: aqueductal stenosis, calf, CT, MRI

Hydrocephalus is defined as enlargement of the cerebral ventricles and subarachnoid space, usually filled with cerebrospinal fluid (CSF) [4]. Many circumstances can expand the ventricles, but the common causes are recognized as interference with the flow or absorption of CSF. Obstructive CSF flow may increase CSF pressure, resulting in enlargement of the cerebral ventricles [4]. This disorder is reported frequently, and results from ischemia, metabolism, trauma, and infections (usually virus) in calves [1, 4, 8, 22]. However, the inheritance of hydrocephalus has been recognized and reported as congenital hydrocephalus [4, 24]. In humans and canines, congenital malformation of the cerebral aqueduct causes occlusion of CSF flow and leads to acquired hydrocephalus, i.e., aqueductal stenosis. In humans, congenital or acquired abnormalities of the mesencephalon have been reported as causing aqueductal stenosis [2, 3, 6, 7, 10, 14, 15, 17, 19, 21]. In particular, a membranous structure in the mesencephalic aqueduct, called "web", sometimes causes aqueductal stenosis and neuro-endoscopic surgery [3, 6, 7, 14, 19]. Aqueductal stenosis caused by hypoplasia of the mesencephalon has been reported in dogs and mice, but no reports in veterinary medicine have described aqueductal stenosis caused by web [4, 17, 24, 25]. Moreover, few reports have described the results of computed tomography (CT) and magnetic resonance imaging (MRI) for the diagnosis of these intracranial malformations in large animal clinical practice, although CT and MRI are used to describe neurological lesions in small animal clinics [12, 22]. Thus, this study reported hydrocephalus with aqueductal stenosis caused by web and characterized the findings using low-field MRI in comparison with findings from normal calves.

A 6-day-old, female Holstein calf weighing 23.5 kg was referred to the Clinic for Large Animals at Rakuno Gakuen University with a history of progressive ataxia at birth. On physical examination, cardiac murmur and doming of the calvaria were observed. Other neurological abnormalities included decreased pupillary light reflex and blindness. Blood examination did not detect bovine viral diarrhea virus, but revealed mild anemia: WBC, 6,000/μl; PCV, 23.4%; TP, 4.6 g/100 m*l*; and PLT, 763,000/μl. We only performed a complete blood count, without biochemical examination, because we suspected intracranial malformation. As a result, we performed CT and MRI under anesthesia. We used intravenous alfaxalone alone (Alfaxan®; Meiji Seika Pharma, Tokyo, Japan) for induction of anesthesia. First, we injected 2 mg/kg of alfaxalone intravenously. We then added alfaxalone intravenously at 0.5 mg/kg twice, because adequate sedation had not been achieved (final dose of alfaxalone, 3 mg/kg). Immediately after induction of

*Correspondence to: Nakade, T.: tnakade@rakuno.ac.jp

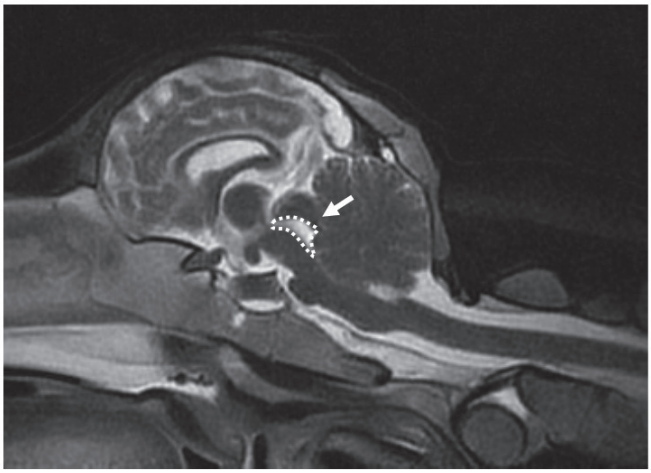

Fig. 1. T2-weighted sagittal MRI in a normal calf. We measured the area of the mesencephalic aqueduct for the anatomical region surrounded by the dotted line (arrow) and evaluated the size of the mesencephalic aqueduct and compared the findings with those from normal calves.

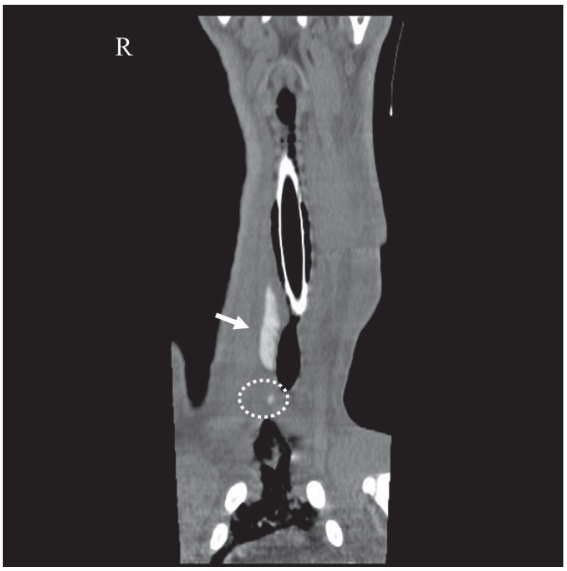

Fig. 2. Lesion of the thyroid lobes on CT. In the thyroid lobes, the right lobe was present between the fourth and fifth cervical vertebrae (arrow). However, the left lobe was not apparent contralaterally, and a thyroid-like structure remained caudal to the right thyroid, located away from the right thyroid gland (dotted line).

anesthesia, we performed tracheal intubation and maintained anesthesia with an end-tidal sevoflurane concentration of 2.0–4.1% (Sevoflo®; Zoetis Japan, Tokyo, Japan) under pure oxygen inhalation. For respiratory management, we used invasive positive pressure ventilation. Multidetector-row CT of the head and neck was performed using a 16-slice CT scanner (Bright Speed Elite 16ch; GE Healthcare, Milwaukee, WI, U.S.A.), and images were acquired at a thickness of 1.25 mm, a table speed of 5.62–17.5 mm/sec and a pitch of 0.562–1.75:1 (120 kV; 133–327 mA). MRI was performed using a 0.2-T open-type scanner (Signa Profile Open Spirit; GE Medical Systems, Milwaukee, WI, U.S.A.). Images included transverse, sagittal and dorsal T2-weighted (first spin echo; repetition time (TR), 3,500–4,000 msec; echo time (TE), 108–119 msec; slice thickness, 5.0–6.5 mm), T1-weighted (TR, 380 msec; TE, 15 msec; thickness, 6.5 mm). These images were evaluated ventricle size in volumetric analysis, according to the method of Esteve-Ratsch *et al* [5]. In volumetric analysis, the lateral ventricle and corresponding hemisphere at the level of interthalamic adhesions were outlined three times and measured using a Digital Imaging and Communications in Medicine (DICOM) Viewer (AZE Virtual Place Lexus, Tokyo, Japan) [5]. These repeated measures were averaged, and ventricle size was calculated as a percentage of hemisphere area [5]. In addition, we used sagittal T2-weighted imaging (T2WI) to evaluate the area of the mesencephalic aqueduct in square millimeters (Fig. 1). To measure and compare ventricle size, six normal Holstein calves with no apparent neurological disease were examined using the same methods applied in the control group.

The cervical vertebrae appeared normal on CT examinations, which showed no dislocation, compression, or spinal instability. However, cervical CT identified morphological abnormalities in the thyroid lobes, with no left thyroid lobe detected. In the thyroid lobes, the location of the right lobe was present between fourth and fifth cervical vertebrae, but the left lobe was not identified on the opposite side. Instead of the left lobe, we observed a structure with the same CT value as the right thyroid lobe, in the caudal right lobe (Fig. 2). Cranial images showed ventricular dilation, particularly of the lateral ventricles, and open fontanelles, but no evidence of cephalic trauma such as skull fracture or cerebral hemorrhage on CT. MR findings for the ventricles and hemisphere area are summarized in Table 1. This case showed marked expansion of the lateral ventricles, especially of the inferior and posterior horns, third ventricle, and mesencephalic aqueduct, but no abnormal intensity in the parenchyma. We observed dorsal displacement of the tectum of the mesencephalon and deformation of the cranial cerebellum by the enlarged mesencephalic aqueduct on sagittal T2-weighted imaging. We could not identify any structures obstructing CSF flow in the mesencephalic aqueduct on sagittal T2-weighted imaging. In the caudal area from the mesencephalic aqueduct, the fourth ventricle and cerebellomedullary cistern appeared normal, so neither an enlarged ventricle nor accumulation of CSF were confirmed. According to volumetric analysis, the percentage of hemisphere occupied by hemi-ventricle was 3.1% (range: 2.2–4.6%) in normal calves, compared to 20.1% in this case. The area of the mesencephalic aqueduct was 48.7 mm^2 (range: 45.7–53.0 mm^2) in normal calves and 92.3 mm^2 in this calf. The mesencephalic aqueduct in this case was more expanded than in normal calves on sagittal T2-weighted imaging (Fig. 3). Although we could not clearly detect the structure, the mesencephalic aqueduct was not straight on dorsal T2-weighted images (Fig. 4). We could not compare the shape of the mesencephalic aqueduct accurately on dorsal T2-weighted images because the form of the structure appeared closer to a domed shape than in normal calves. However, the mesencephalic aqueduct showed a midline shift to the right side, and was enlarged compared to normal calves. As an additional

Table 1. The size of the ventricle area and the mesencephalic aqueduct

Group	Number	Sex	Age (days old)	Percentage of ventricle area	Mesencephalic aqueduct (mm^2)
Normal	1	Female	14	4.6	53.0
Normal	2	Female	14	3.1	46.3
Normal	3	Male	28	2.9	52.3
Normal	4	Male	7	2.9	48.7
Normal	5	Male	28	2.6	46.0
Normal	6	Male	56	2.2	45.7
Average			24.5	3.1	48.7
Case		Female	6	20.1	92.3

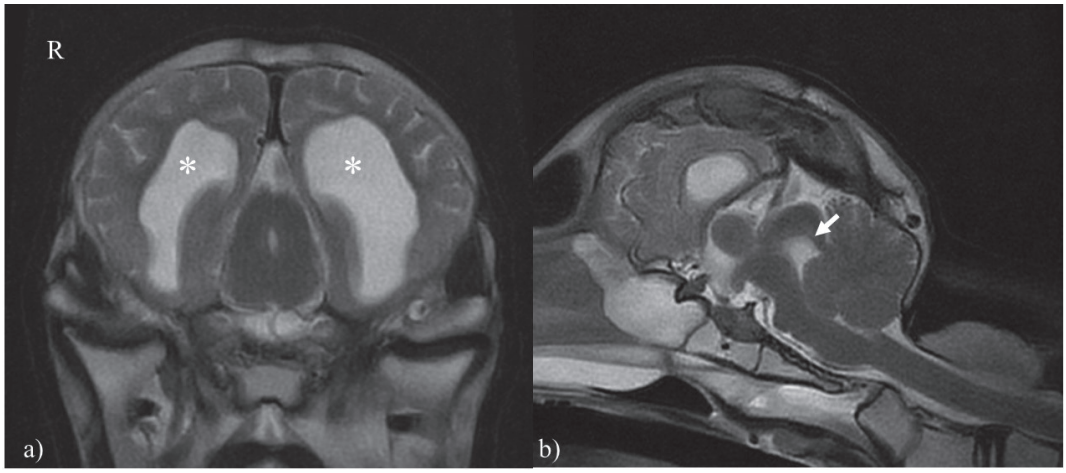

Fig. 3. The lesion on transverse (a) and sagittal (b) T2-weighted images in this case. Lateral ventricles (*) and the mesencephalic aqueduct were expanded and compressed the cerebrum and rostral cerebellum (arrow).

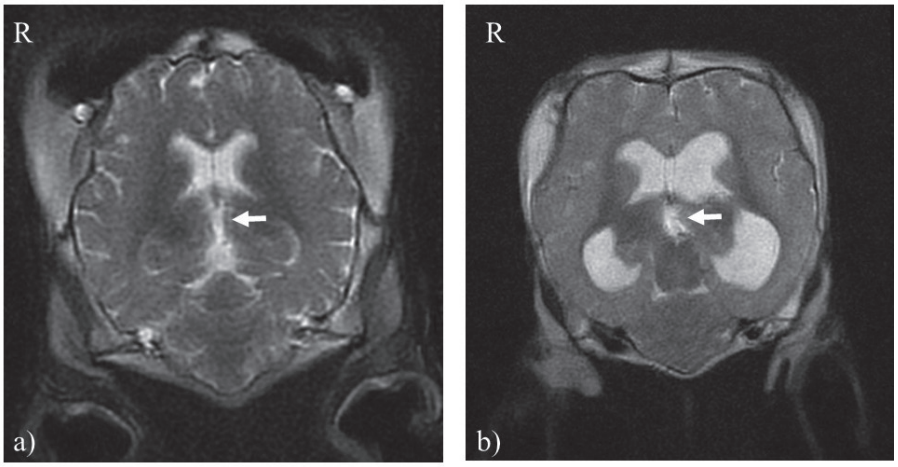

Fig. 4. (a) Dorsal T2WI in a normal calf. (b) Dorsal image on T2WI in this case. The structure in the mesencephalic aqueduct was not clearly described, but the aqueduct was not straight on dorsal T2WI (arrow) in the case compared with a normal calf.

finding, the sulcus of the cerebrum was more indistinct because of the enlarged ventricle than in normal cases; in particular, the lateral ventricle was markedly extended. After CT and MRI, the calf underwent ultrasonography to evaluate cardiovascular anomalies, revealing ventricular septal defect, atrial septal defect, and aortic overriding. Neurological signs were deteriorated compared to before examination. Before anesthesia, the calf was able to stand with assistance, but after anesthesia, the calf tried to stand but could not. Three days after the examination, the calf no longer wanted to stand, so we decided to perform euthanasia and

postmortem examination. Gross examination revealed that the lateral ventricles were enlarged and the cerebral parenchyma was markedly atrophied. In addition, an abnormal structure like a membrane was identified in the caudal mesencephalic aqueduct, despite not being apparent on MRI (Fig. 5). The structure was thin, whitish, and looked like a membrane, with no distribution of blood vessels. We also could not observe any redness or hyperplasia of the structure and mesencephalic aqueduct. The mesencephalic aqueduct was not covered completely by the structure, so partial flow of CSF into the mesencephalic aqueduct was confirmed. Other skeletal abnormalities included cleft palate, curved body of the mandible, and spinal curvature between the 7th and 9th thoracic vertebrae. Furthermore, disseminated pulmonary congestion and nephredema associated with cardiac failure were apparent. We therefore diagnosed this case as congenital hydrocephalus caused by aqueductal stenosis. We considered the other congenital abnormalities as incidental findings.

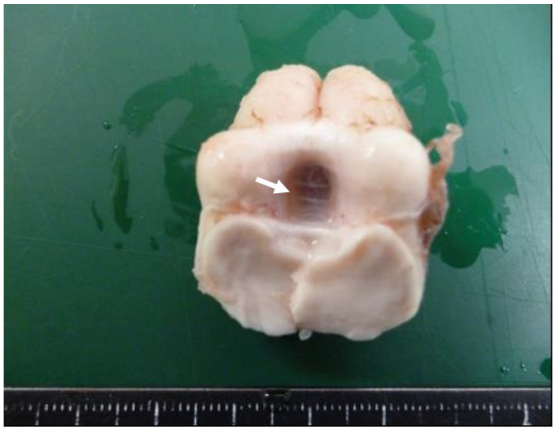

Fig. 5. Pathological findings of an abnormal, membrane-like structure in the caudal mesencephalic aqueduct (arrow).

Hydrocephalus represents ventricular dilation with CSF accumulation, and the many causes that have been described all resulted in interference with the flow or absorption of CSF. Developmental obstructive hydrocephalus is a well-known congenital malformation in dogs [4, 17, 25]. The characteristic clinical findings in most dogs with hydrocephalus include 'dome-shaped' calvaria, open fontanelles, divergent strabismus, and growth retardation [4, 17]. In addition, neurological findings were progressive ataxia, seizures, and somnolence, causing abnormality of the forebrain due to dilation of the ventricles [4, 17]. The abnormal features in this calf resembled those seen in dogs, and decreased pupillary light reflex and blindness had been identified in neurological examination. This is because marked enlargement at the posterior horn of the lateral ventricle and the mesencephalic aqueduct affect the occipital lobe and mesencephalon, respectively [4]. The anatomical abnormalities from accumulated CSF were clearly observed on MRI, and a great preponderance of the ventricles was also evident from volumetric analyses. Volumetric analysis offered MR images resembling those shown in a recent report in dogs; the ratio of ventricle area to crania was 3.1%, the same range seen in normal dogs [5]. In dogs, revealing the differences between symptomatic hydrocephalus and asymptomatic hydrocephalus from MRI alone is sometimes difficult [4, 5, 11, 20]. However, in this calf, the neurological abnormalities of blindness and ataxia were consistent with the most expanded and affected ventricle area. Volumetric analysis, compared with results from normal calves, thus appears to enable objective evaluation of the range of dilation with CSF accumulation.

In addition, MRI in this case showed that the lateral ventricles, third ventricle, and mesencephalic aqueduct were markedly expanded despite the normal fourth ventricle. Compared with normal calves, the mesencephalic aqueduct appeared markedly expanded in this calf and caused dorsal displacement of the tectum of mesencephalon and deformation of the cranial cerebellum on MRI. Generally, in cattle, some viral infections are known to cause dilation of the lateral ventricles [1, 4]. However, hydrocephalus due to viral infections (i.e., BVD and Akabane viral infections) are characterized by a loss of parenchyma [1, 4, 8]. These viral infections damage neuronal cells directly and cause inflammatory responses, leading to hypoplasia and atrophy of the parenchyma. As a result, CSF is accumulated to compensate for the space of the hypoplasia in a process called compensatory hydrocephalus [4]. In this case, we could not observe hypoplasia or atrophy in the cerebral parenchyma, and no abnormal MR findings indicated inflammation. Hydrocephalus characterized by partial ventricular dilation as in this case may lead to a suspicion of obstructive hydrocephalus, not compensatory hydrocephalus [4]. MRI findings resembled those seen in other animals and humans with hydrocephalus caused by interference with CSF flow at the mesencephalic aqueduct [2–4, 6, 7, 10, 14–17, 19, 21, 24]. Generally, disturbance of CSF flow at the mesencephalic aqueduct such as in aqueductal stenosis is diagnosed by findings of considerable expansion of the lateral ventricles, third ventricle, while the fourth ventricles remain normal [2–4, 6, 7, 10, 14–17, 19]. Feline infectious peritonitis is a good example of acquired obstructive hydrocephalus in the mesencephalic aqueduct, which may cause local expansion of the lateral and third ventricles [4, 16]. Although the site of occlusion varies depending on the site of inflammation, when the occlusion occurs in mesencephalic aqueduct, expansion of the lateral and third ventricles and findings of a normal fourth ventricle are obtained [4, 16]. Similarly, malformation of the mesencephalon causing aqueductal stenosis, which is called developmental obstructive hydrocephalus, may lead to dilation of the lateral and third ventricles with CSF accumulation [4, 24]. This malformation is known to show recessive inheritance in mice [24]. These abnormalities at the mesencephalic aqueduct are due to dysplasia of the mesencephalon comprising a fused or undivided rostral or caudal colliculus [4, 24]. Since these abnormalities at the mesencephalon cause occlusion of the mesencephalic aqueduct, confirming the mesencephalic aqueduct even under pathological autopsy is often difficult. However, expansion of the mesencephalic aqueduct was also clear on sagittal T2WI in this calf, especially in the marked expansion of the mesencephalic aqueduct followed by sudden narrowing of the entrance to the fourth ventricle. In humans, as a report showing findings similar to this calf, a structure called "web" is known to form in the mesencephalic aqueduct, whereby expansion of the lateral ventricles, third ventricle and mesencephalic aqueduct can be recognized in some human cases [7]. While the fourth ventricle is normal, accumulation of CSF at the mesencephalic aqueduct and displacement of the tectum of the mesencephalon may result [7]. We observed dorsal displacement of the tectum of

the mesencephalon in this calf, too. In addition to these findings, aquedactal stenosis by the web is diagnosed from MR findings, with no obvious abnormalities in the parenchyma, but presence of a membrane-like structure in the mesencephalic aqueduct [3, 6, 7, 14, 15]. The images on dorsal T2WI may confirm the structure in the mesencephalic aqueduct, but did not in this case [6]. However, compared with normal calves, the mesencephalic aqueduct displayed a midline shift to the right side. Such findings have not been reported in humans, but perhaps could be seen as a partial volume effect as a result of the combination of the structure, expansion and sudden stenosis of the mesencephalic aqueduct. We could not describe any structures in the mesencephalic aqueduct on MRI, but the findings of secondary changes such as partial expansions of the ventricles, displacement of the tectum of the mesencephalon, and normal parenchyma were consistent with findings from previous reports [3, 6, 7, 14, 15]. A finding of secondary changes by web may thus be useful for diagnosis even if the structure is present at the mesencephalon.

According to Matsuda *et al*, fast imaging employing steady-state (FIESTA) sagittal and dorsal acquisition is necessary to describe a thin septum [14]. Moreover, measurement of CSF flow by high-field MRI is reportedly useful to evaluate treatment and follow-up after surgery [10, 19]. Description of aqueductal CSF flow using 3-dimensional heavily T2-weighted sequences should reportedly enable detection of thin structures at the mesencephalic aqueduct [10]. Unfortunately, in veterinary medicine, the mesencephalon is not generally imaged using those sequences, because malformed mesencephalon caused by web has not been reported. Web consists of a thin ependymal septum, and the cause of formation is unknown because there are few cases in humans and veterinary medicine [3, 6, 14, 15]. This calf did not have BVD and the results of MRI were normal in the parenchyma at least, so congenital aqueductal stenosis by web was diagnosed in postmortem examination. Because there is a possibility that congenital or acquired aqueductal stenosis by web, we should perform evaluations carefully and add thin slice sequences when MR images show considerable expansion of the lateral ventricles, third ventricle, and mesencephalic aqueduct despite a normal appearance of the fourth ventricle.

In addition to MRI, CT and ultrasonography revealed thyroid dysplasia and cardiovascular anomalies in this case, but these findings were not considered relevant to the aqueductal stenosis. In humans, patients with Fanconi's anemia sometimes show multiple malformations, such as hydrocephalus and hypoplasia of almost all endocrine grands, including the pituitary and thyroid [13]. Such patients often display dwarfism and an absence of pigmentation because of the congenital hypopituitarism. However, the pituitary in this case was normal on MRI and no reports have described a relationship between aqueductal stenosis and either dysplasia of the thyroid or cardiovascular anomalies in veterinary medicine, so we considered this case as representing dysplasia of the thyroid gland with incidental cardiovascular anomalies. Although the causes of the multiple congenital malformations were unclear, CT was helpful as a screening examination to detect these other abnormalities. In this case, the blood biochemistry and hormone data (T3, T4 and thyroid-stimulating hormone) were not obtained because we suspected intracranial disease. Consideration of these examinations together we might not only allow visualization of structural abnormalities, but also qualitative change.

On the other hand, CT and MRI require anesthesia, which increases the cost and is restricted to limited locations. Some reports from canines have indicated that ultrasonography of the hydrocephalus reflects the intracranial condition [9, 11, 18, 20]. According to Tsuka *et al.*, transorbital echoencephalography is useful to detect hydrocephalus and hydranencephalus in cattle [23]. However, describing the ventricles is sometimes difficult, because calves move during examinations in the absence of anesthesia. In addition, the aqueduct is located caudal to the lateral ventricles, so the anatomical location may contribute to the difficulty in describing the structure in the mesencephalon.

In conclusion, this report suggests that congenital aqueductal stenosis can be caused by web in calves, as in humans. In this study, web was not visualized by spin echo sequences, but was described by a gradient-echo sequence. Hydrocephalus should therefore be diagnosed with care, especially when we observe MR images showing considerable expansion of the lateral ventricles, third ventricle, and mesencephalic aqueduct, while the fourth ventricles remain normal, because structures in the mesencephalic aqueduct may obstruct CSF flow by web. CT and MRI are useful to describe mesencephalic aqueductal stenosis by web and to detect other malformations for antemortem diagnosis.

REFERENCES

1. Agerholm, J. S., Hewicker-Trautwein, M., Peperkamp, K. and Windsor, P. A. 2015. Virus-induced congenital malformations in cattle. *Acta Vet. Scand.* **57**: 54–67. [Medline] [CrossRef]
2. Akhondi, H., Barochia, S., Holmström, B. and Williams, M. J. 2003. Hydrocephalus as a presenting manifestation of neurosarcoidosis. *South. Med. J.* **96**: 403–406. [Medline] [CrossRef]
3. Algin, O., Hakyemez, B. and Parlak, M. 2010. Phase-contrast MRI and 3D-CISS versus contrast-enhanced MR cisternography on the evaluation of the aqueductal stenosis. *Neuroradiology* **52**: 99–108. [Medline] [CrossRef]
4. Delahunta, A., Glass, E. and Kent, M. Neuroanatomy gross description and atlas of transverse sections and magnetic resonance images. pp. 60–101. *In*: Veterinary neuroanatomy and clinical neuology, 4th ed., Sunders, Philadelphia.
5. Esteve-Ratsch, B., Kneissl, S. and Gabler, C. 2001. Comparative evaluation of the ventricles in the Yorkshire Terrier and the German Shepherd dog using low-field MRI. *Vet. Radiol. Ultrasound* **42**: 410–413. [Medline] [CrossRef]
6. Flora, N., Kulasekaran, N., Mudali, S. K. and Swaminathan, T. S. 2005. Compensated aqueduct of sylvius obstruction by web-a case report. *Indian J. Radiol. Imaging* **15**: 19–20. [CrossRef]
7. Gökalp, H. Z. and Tascioglu, A. O. 1977. Membranous occulusion of the aqueduct of Sylvius. *Surg. Neurol.* **8**: 103–105. [Medline]
8. Greene, H. J., Leipold, H. W. and Hibbs, C. M. 1974. Bovine congenital defects: variations of internal hydrocephalus. *Cornell Vet.* **64**: 596–616. [Medline]
9. Hudson, J. A., Simpson, S. T., Buxton, D. F., Cartee, R. E. and Steiss, J. E. 1990. Ultrasonographic diagnosis of canine hydrocephalus. *Vet. Radiol.*

31: 50–58. [CrossRef]
10. Kartal, M. G. and Algin, O. 2014. Evaluation of hydrocephalus and other cerebrospinal fluid disorders with MRI: An update. *Insights Imaging* **5**: 531–541. [Medline] [CrossRef]
11. Kii, S., Uzuka, Y., Taura, Y., Nakaichi, M., Takeuchi, A., Inokuma, H. and Onishi, T. 1997. Magnetic resonance imaging of the lateral ventricles in beagle-type dogs. *Vet. Radiol. Ultrasound* **38**: 430–433. [Medline] [CrossRef]
12. Lee, K., Yamada, K., Tsuneda, R., Kishimoto, M., Shimizu, J., Kobayashi, Y., Furuoka, H., Matsui, T., Sasaki, N., Ishii, M., Inokuma, H., Iwasaki, T. and Miyake, Y. 2009. Clinical experience of using multidetector-row CT for the diagnosis of disorders in cattle. *Vet. Rec.* **165**: 559–562. [Medline] [CrossRef]
13. London, R., Drukker, A. and Sandbank, U. 1965. Fanconi's anaemia with hydrocephalus and throid abnormality. *Arch. Dis. Child.* **40**: 89–92. [Medline] [CrossRef]
14. Matsuda, M., Shibuya, S., Oikawa, T., Murakami, K. and Mochizuki, H. 2011. [A case of late-onset aqueductal membranous occlusion and a successful treatment with neuro-endoscopic surgery]. *Rinsho Shinkeigaku* **51**: 590–594 (in Japanese). [Medline] [CrossRef]
15. Mohammed, H., Elsatar, A. B. A., Ragab, M. and Alghriany, A. 2016. Evaluation of late onset congenital aquedactal stenosis hydrocephalus. *J. Neurol. Stroke* **5**: 163–169. [CrossRef]
16. Okada, M., Kitagawa, M., Ito, D., Itou, T., Kanayama, K. and Sakai, T. 2009. MRI of secondary cervical syringomyelia in four cats. *J. Vet. Med. Sci.* **71**: 1069–1073. [Medline] [CrossRef]
17. Sahar, A., Hochwald, G. M., Kay, W. J. and Ransohoff, J. 1971. Spontaneous canine hydrocephalus: cerebrospinal fluid dynamics. *J. Neurol. Neurosurg. Psychiatry* **34**: 308–315. [Medline] [CrossRef]
18. Saito, M., Olby, N. J., Spaulding, K., Muñana, K. and Sharp, N. J. H. 2003. Relationship among basilar artery resistance index, degree of ventriculomegaly, and clinical signs in hydrocephalic dogs. *Vet. Radiol. Ultrasound* **44**: 687–694. [Medline] [CrossRef]
19. Schroeder, H. W., Oertel, J. and Gaab, M. R. 2004. Endoscopic aqueductoplasty in the treatment of aqueductal stenosis. *Childs Nerv. Syst.* **20**: 821–827. [Medline] [CrossRef]
20. Spaulding, K. A. and Sharp, N. J. H. 1990. Ultrasonographic imaging of the lateral cerebral ventricles in the dog. *Vet. Radiol.* **31**: 59–64. [CrossRef]
21. Stoquart-El Sankari, S., Lehmann, P., Gondry-Jouet, C., Fichten, A., Godefroy, O., Meyer, M. E. and Baledent, O. 2009. Phase-contrast MR imaging support for the diagnosis of aqueductal stenosis. *AJNR Am. J. Neuroradiol.* **30**: 209–214. [Medline] [CrossRef]
22. Tsuka, T. and Taura, Y. 1999. Abscess of bovine brain stem diagnosed by contrast MRI examinations. *J. Vet. Med. Sci.* **61**: 425–427. [Medline] [CrossRef]
23. Tsuka, T., Okamura, S., Nakaichi, M., Une, S. and Taura, Y. 2002. Transorbital echoencephalography in cattle. *Vet. Radiol. Ultrasound* **43**: 55–61. [Medline] [CrossRef]
24. Vogel, P., Read, R. W., Hansen, G. M., Payne, B. J., Small, D., Sands, A. T. and Zambrowicz, B. P. 2012. Congenital hydrocephalus in genetically engineered mice. *Vet. Pathol.* **49**: 166–181. [Medline] [CrossRef]
25. Wünschmann, A. and Oglesbee, M. 2001. Periventricular changes associated with spontaneous canine hydrocephalus. *Vet. Pathol.* **38**: 67–73. [Medline] [CrossRef]